Correlation for the effective gas diffusion coefficient in carbon paper diffusion media

Zamel, Nada; Li, Xianguo; Shen, Jun

Publisher's version / Version de l'éditeur:
https://doi.org/10.1021/ef900653x
Energy & Fuels, 23, 12, pp. 6070-6078, 2009-10-23

Energy Fuels **2009,** *23,* 6070–6078 · DOI:10.1021/ef900653x
Published on Web 10/23/2009

energy&fuels
article

Correlation for the Effective Gas Diffusion Coefficient in Carbon Paper Diffusion Media

Nada Zamel,[†] Xianguo Li,*[,†] and Jun Shen[‡]

[†]*20/20 Laboratory for Fuel Cells and Green Energy RD&D, Department of Mechanical and Mechatronics Engineering, University of Waterloo, Waterloo, ON, Canada, and* [‡]*Institute for Fuel Cell Innovation National Research Council, Vancouver, BC, Canada*

Received June 28, 2009. Revised Manuscript Received September 18, 2009

The understanding of mass transport limitations in polymer electrolyte membrane (PEM) fuel cells is crucial in the research and progress of this technology. The structure of the components, specifically the as diffusion layer (GDL), of PEM fuel cells, is complex. Thus, for the purpose of simulating mass transport in the GDL, the effect of the structure on the diffusion coefficient is taken into account by introducing an effective diffusion coefficient. The effective diffusion coefficient of a gas is lower than its corresponding bulk diffusion coefficient due to the presence of a solid matrix in the porous materials. Currently, the Bruggeman approximation is the most widely used correlation for estimating the effective diffusion coefficient in the GDL. Other semiempirical models are also available. However, these correlations overestimate the effective diffusion coefficient due to the assumptions on which they are based. In this study, correlations for the through-plane and in-plane diffusibility in the GDL are developed based on a three-dimensional (3D) simulation of gas diffusion in the GDL. The 3D structure of the TORAY carbon paper with no binding material is reconstructed using stochastic models and used as the modeling domain. The numerical results are shown to have a good agreement with experimental data of diffusibility in both directions. Correlations for two different porosity ranges are given.

Introduction

Much of the transport phenomena encountered in engineering applications occur through porous media. Porous materials are made up of two different parts, the solid matrix and the void space. The void space is normally occupied by one or more fluid phases, with each of these phases occupying a distinct portion of the void space. Despite the similarity in composition of the natural and artificial occurring porous materials, their geometries vary tremendously depending on their applications. This variation can in turn affect the overall trend of the transport phenomena. In this study, carbon paper, shown in Figure 1, is the porous material under investigation. Carbon paper is used in polymer electrolyte membrane (PEM) fuel cells for the transport of gases and electrons to the reaction sites and is commonly referred to as the gas diffusion layer (GDL).

As seen from the scanning electron microscope (SEM) images of a carbon paper sample, the structure of carbon paper is very complex. As the name suggests, carbon paper is manufactured from carbon powder. Three distinct regions exist with the two main regions being the solid and void regions. The solid matrix consists of long, thin fibers, that are randomly distributed. These fibers are good electron conductors; hence they are used to transport electrons to and from the catalyst layer. The void region is used as the medium for fluid transport in the gas and/or liquid phase. The last region appears as a thin binder, which binds the fibers of the paper. This binder is also made from a carbon composite and does not play a part in any transport phenomenon. The binder is used to enhance the durability and strength of carbon paper, preventing the fibers from cracking. The structure of this binding material changes drastically once carbon paper is treated with Teflon as shown in Figure 2a, becoming a highly hydrophobic area as suggested by Figure 2b. Figure 2b shows the distribution of fluorine on carbon paper after the Teflon treatment. Teflon is used to make carbon paper hydrophobic; hence, assisting in liquid water removal.

The structure of carbon paper is further complicated by its anisotropic nature. An SEM image of a cross section of a carbon paper sample, Figure 3, reveals the configuration of the fibers in the in-plane direction. The fibers run perpendicular to the thickness of the paper. This further complication of the structure can affect the overall mass transport in this type of medium.

As mentioned earlier, carbon paper is used as GDL in PEM fuel cells. The progress in the research and development of these cells depends heavily on the understanding of the transport phenomena in the cells. However, due to the complexity of monitoring species transport experimentally, mathematical models are often used to investigate this transport and they are abundant in the literature.[1−3] The diffusion of gases in the porous gas diffusion layer is an important determinant, especially at high current densities, of the transport of species in PEM fuel cells. However, it is very computationally expensive to model the real structure of the GDL when the other components of the cell are also being considered. Thus, correction factors are normally used to account for the structural effects on the gas diffusion coefficient of gases in the GDL. Currently, the Bruggeman's correction factor[4] is the most widely used correlation to obtain the effective diffusion coefficient of gases in the GDL. The relation was derived using effective medium approximations,

*To whom correspondence should be addressed. E-mail: x6li@uwaterloo.ca.

(1) Weber, A. Z.; Newman, J. *Chem. Rev.* **2004**, *104*, 4679–4726.
(2) Cheddie, D; Munroe, N. *J. Power Sources* **2005**, *142*, 72–84.
(3) Biyikoglu, A.; Int, J. *Hydrogen Energy* **2005**, *30*, 1181–1212.
(4) Bruggeman, D. A. G. *Ann. Phys.* (*Leipzig*) **1935**, *24*, 636–664.

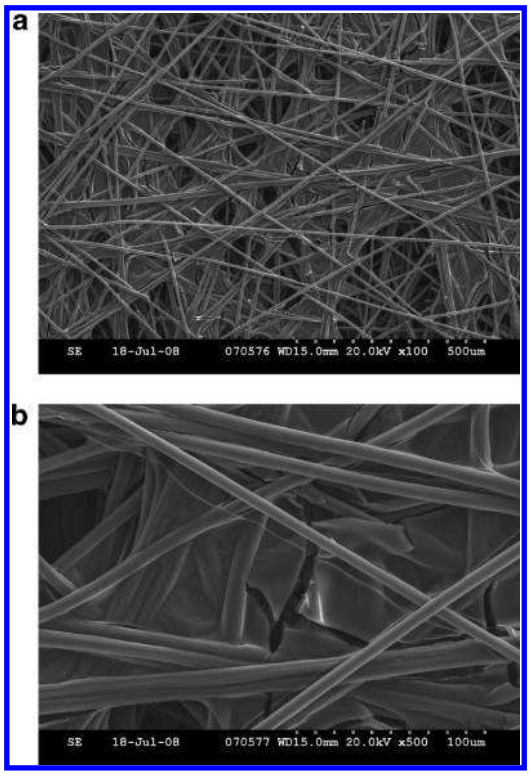

Figure 1. Scanning electron microscope images of TORAY carbon paper (TPGH-120) with 0% Teflon treatment with different magnifications: (a) 100, (b) 500.

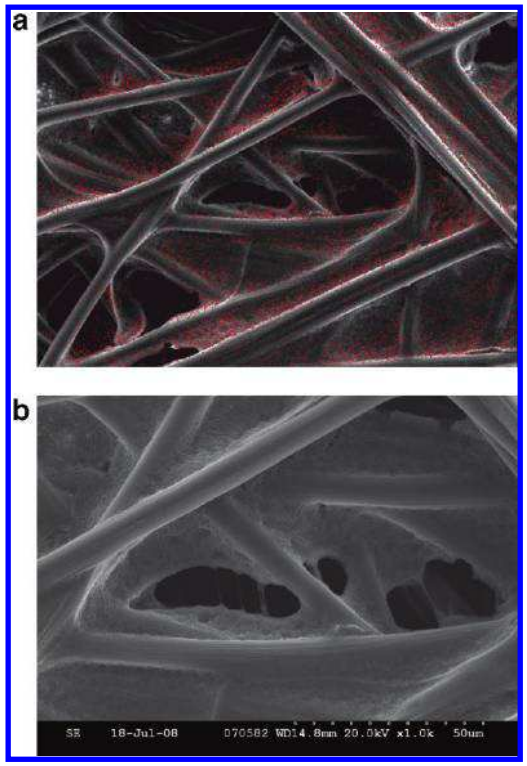

Figure 2. Images of TORAY carbon paper (TPGH-120) with 30% by weight Teflon treatment (a) scanning electron microscope image; (b) fluorine distribution shown with red dots.

which are analytical models used to describe macroscopic properties of porous media. These approximations sometimes do not apply to percolating systems; thus, failing to accurately estimate their properties. The Bruggeman approximation was

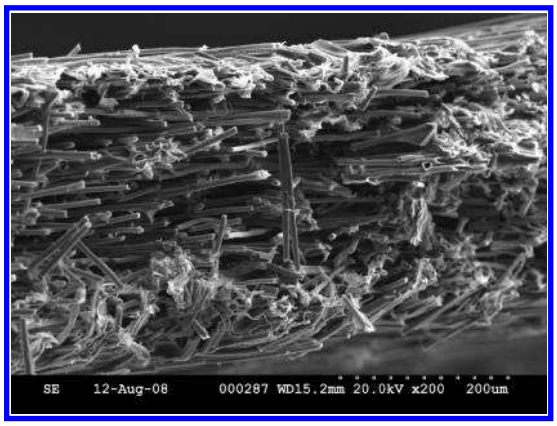

Figure 3. Scanning electron microscope image of a cross section of TORAY carbon paper (TPGH-120) with no Teflon treatment.

derived for electrical conductivity and the dielectric constant of a medium composed of uniformly distributed spheres. Effective transport relations are sometimes interchangeable; thus, the Bruggeman approximation in terms of the diffusion coefficients has been commonly written as:[4]

$$\frac{D_{\text{eff}}}{D_{\text{bulk}}} = \varepsilon^{m} \tag{1}$$

where m is the Bruggeman exponent, and its widely used value is 1.5; D_{eff} is the effective diffusion coefficient; D_{bulk} is the bulk diffusion coefficient; and ε is the porosity.

Other attempts for correlating the effective diffusion coefficient to the bulk diffusion coefficient in porous media are found in refs 5−8. Neale and Nader[5] developed an expression for an isotropic porous medium composed of spherical particles as follows:

$$\frac{D_{\text{eff}}}{D_{\text{bulk}}} = \left(\frac{2\varepsilon}{3-\varepsilon}\right) \tag{2}$$

The expression in eq 2 was developed mathematically for a homogeneous and isotropic swarm of impermeable spheres with a porosity, ε, and an arbitrary size distribution. In order to develop the expression, an arbitrary sphere with a radius, R, and its associated pore space having a radius, S, are used. The outer radius of the pore space is chosen in such a way that the porosity of the unit cell (reference sphere and the concentric shell) is identical to that of the original system. In order to satisfy this constraint, Neale and Nader[5] suggested that:

$$\frac{S}{R} = (1-\varepsilon)^{-1/3} \tag{3}$$

which should hold for the porosity range $0 \leq \varepsilon \leq 1$

In the study by Das et al.,[8] they used a mathematical formulation of the Hashin coated sphere model to obtain the effective diffusion coefficient in the GDL of PEM fuel cells. The expression they found resembles that by Neale and Nader,[5] eq 2, and is given as:

$$\frac{D_{\text{eff}}}{D_{\text{bulk}}} = \left(1-\left(\frac{3(1-\varepsilon)}{3-\varepsilon}\right)\right) \tag{4}$$

It should be pointed out here that the expression given by eq 4 provides an upper bound for the effective diffusion coefficient.

(5) Neale, G. H.; Nader, W. K. *AIChE J.* **1973**, *19*, 112–119.
(6) Tomadakis, M. M.; Sotirchos, S. V. *AIChE J.* **1993**, *39*, 397–412.
(7) Nam, J. H.; Kaviany, M. *Int. J. Heat Mass Transfer* **2003**, *46*, 4595–4611.
(8) Das, P. K.; Li, X; Liu, Z. S. *Applied Energy* **2009**. (doi:10.1016/j.apenergy.2009.05.006).

This upper bound is formulated for porous media with spherical particles without taking into account certain statistical parameters of the random geometry.[9] Das et al.[8] argued that in order to take the statistical randomness of the geometry as well as the structure of the solid matrix into account, a function, $f(\varepsilon)$, should be introduced to their expression as follows:

$$D_{\text{eff}}^{\text{dry}} = D_{\text{bulk}}\left(1 - f(\varepsilon)\left(\frac{3(1-\varepsilon)}{3-\varepsilon}\right)\right) \quad (5)$$

where $f(\varepsilon) \geq 0$ and could vary depending on the geometry of the solid matrix.

The correlation of the effective diffusion coefficient in porous media obtained by Tomadakis and Sotirchos[6] was based on the general percolation theory and random distribution of fibers in a porous medium. They used a Monte Carlo scheme to determine the effective diffusion coefficient of randomly placed molecules in the interior of a porous structure. Their scheme was employed to study the effect of the dimensionality of the structure (i.e., $d = 1$, 2, and 3) as well as the Knudsen number. The expression developed for molecular diffusion is as follows:

$$\frac{D_{\text{eff}}}{D_{\text{bulk}}} = \varepsilon\left(\frac{\varepsilon-\varepsilon_{\text{p}}}{1-\varepsilon_{\text{p}}}\right)^{\alpha} \quad (6)$$

where ε_{p} is a percolation threshold, and α is an empirical constant. Typical value for the percolation threshold is 0.037, and the empirical constant is 0.661 for the three-dimensional (3D) porous media. The parameter values for one-dimensional (1D) and two-dimensional (2D) cases for each directionality and diffusion direction were provided in literature.[6] The expression in eq 6 was compared against experimental data for diffusion in sand with various packing and showed very good agreement with experimental data. However, the validity of this expression for estimating the effective diffusion coefficient in the GDL of PEM fuel cells is still questionable because of the significantly different geometries involved. First, it has not been verified against experimental data for diffusion in the GDL. Second, the expression for the 3D porous material assumes that the material is isotropic, which is not true in the case of carbon paper.

The expression by Nam and Kaviany[7] could be considered as an extension to the expression by Tomadakis and Sotirchos.[6] It was also derived from the percolation theory and extended to consider the effect of liquid water condensation on the diffusion process. They assumed that the GDL is made up of stacked 2D random carbon fiber mats. They assumed that the fibers are infinitely long in the x and y directions, the in-plane direction, and are allowed to overlap. The solid structure is modeled as stacks of continuously overlapping fiber screens.

Using the percolation theory to develop a correlation for the effective diffusion coefficient, they found the effective diffusivity as a function of porosity and liquid water saturation to be:

$$\frac{D_{\text{eff}}}{D_{\text{bulk}}} = \varepsilon\left(\frac{\varepsilon-0.11}{1-0.11}\right)^{0.785} \quad (7)$$

Again, the correlation given in eq 7 was not compared to experimental data and simplifications were made in regards to the geometry of the GDL. Similar geometry is adopted for the GDL in a study by Gostick et al.[10] to understand the behavior of the relative permeability and gas diffusion for different saturation levels. According to the results of their numerical simulation, Gostick et al.[10] argued that many of the available correlations overpredict the effective parameters of the GDL. Their findings also followed a percolation type behavior; however, they did not state a specific correlation for their findings. Their findings are very similar to those calculated by the expression from the study by Nam and Kaviany.[7]

It is then apparent that many models are available for obtaining the effective diffusion coefficient in the GDL. However, due to the geometry differences and the lack of experimental data for comparison, it becomes difficult to choose the most appropriate correlation. In recent years, estimating the effective diffusion coefficient, both experimentally and numerically, of gases in carbon paper has gained much interest. Using the limiting current density, Baker et al.[11] estimated the effective diffusion coefficient of an oxygen−nitrogen mixture through a TORAY carbon paper sample. They used Fick's law to relate the limiting current density to the effective diffusion coefficient as given below:[11]

$$D_{\text{O}_2}^{\text{eff}} = \left(\frac{fhi_{\text{lim}}RT}{4FP_{\text{O}_2}^{\text{in}}}\right) \quad (8)$$

where $D_{\text{O}_2}{}^{\text{eff}}$ is the effective diffusion coefficient of oxygen in nitrogen in carbon paper, f is a geometrical factor, h is the thickness of carbon paper, i_{lim} is the limiting current density, R is the universal gas constant, T is the temperature, F is Faraday's constant, and $P_{\text{O}_2}{}^{\text{in}}$ is the partial pressure of oxygen at the channel/carbon paper interface.

Kramer and co-workers[12,13] measured the effective diffusion coefficient in carbon paper using electrochemical impedance spectroscopy. Electrochemical impedance spectroscopy is applied to measure the effective ionic conductivity of an electrolyte-soaked carbon paper sample. The effective diffusion coefficient is then found using the analogy between Ficks and Ohms laws. In their early study,[12] they measured the effective diffusion coefficient through TORAY carbon paper with no wet-proofing. In their second study,[13] they measured the effective diffusion coefficient through TORAY and SGL carbon paper with different Teflon percentage. The impact of wet proofing on the effective diffusion coefficient was also investigated experimentally in our previous study.[14]

In a study by Schulz et al.,[15] the stochastic simulation technique was used to create a 3D reconstruction of carbon paper, which was proposed by Schladitz et al.[16] and is based on a Poisson line process with one-parametric directional distribution where the fibers are realized as circular cylinders with a given diameter. In the study by Schulz et al.,[15] they investigated the two-phase flow in the gas diffusion layer. In

(9) Weissberg, H. L. *J. Appl. Phys.* **1963**, *34*, 2636–2639.

(10) Gostick, J. T.; Ioannidis, M. A.; Fowler, M. W.; Pritzker, M. D. *J. Power Sources* **2007**, *173*, 277–290.

(11) Baker, D; Wieser, C; Neyerlin, K. C.; Murphy, M. W. *ECS Trans.* **2006**, *3*, 989–999.

(12) Kramer, D; Freunberger, S. A.; Flückiger, R; Schneider, I. A.; Wokaun, A; Büchi, F. N.; Scherer, G. G. *J. Electroanal. Chem.* **2008**, *612*, 63–77.

(13) Flückiger, R; Freunberger, S. A.; Kramer, D; Wokaun, A; Scherer, G. G.; Büchi, F. N. *Electrochim. Acta* **2008**, *54*, 551–559.

(14) Zamel, N.; Astrath, N. G. C.; Li, X; Shen, J.; Zhou, J.; Astrath, F. B. G.; Wang, H.; Liu, Z. S. *Chem. Eng. Sci.* **2009**. (doi:10.1016/j.ces.2009.09.044).

(15) Schulz, V. P.; Becker, J; Wiegmann, A; Mukherjee, P. P.; Wang, C. Y. *J. Electrochem. Soc.* **2007**, *154*, B419–B426.

(16) Schladitz, K; Peters, S; Reinel-Bitzer, D; Wiegmann, A; Ohser, J. *Comput. Mater. Sci.* **2006**, *38*, 56–66.

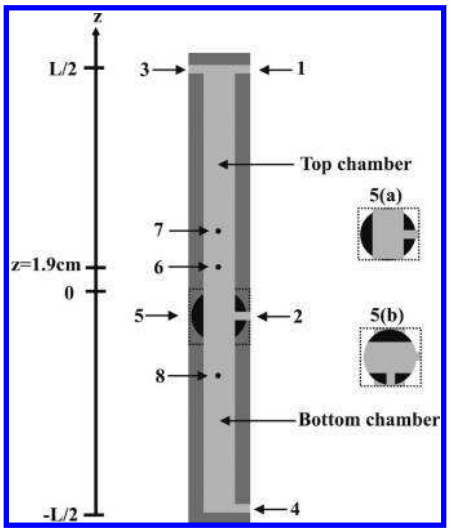

Figure 4. Schematic diagram of a diffusion cell. 1: gas inlet 1; 2: gas inlet 2; 3 and 4: outlets; 5: a ball valve; 5(a): open position of valve; 5(b): closed position of valve; 6: oxygen sensor; 7 and 8: humidity sensors.

later studies,[17,18] the same group continued their investigation of liquid water transport and its effects on the overall diffusion process of gases in the GDL. Much of the work done in this area is summarized in the book chapter by Mukherjee and Wang.[19]

Despite the fact that many of these studies mentioned above have been focused on estimating the effective diffusion coefficient in carbon paper, they did not generate a specific correlation for this diffusion coefficient to be used in numerical simulation of the transport phenomena in the GDL. The objective of the investigation presented in this paper is to obtain a correlation for the effective diffusion coefficient of gases in dry carbon paper. The numerical results of this study compared to experimental data will be used for this purpose.

Experimental Setup

In our previous study,[14] the through-plane effective diffusion coefficient of a humidified oxygen−nitrogen mixture was measured using a Loschmidt cell apparatus, shown in Figure 4. A Loschmidt cell consists of two chambers filled with two different gases, separated with a partition. Upon the removal of the partition, the two gases are allowed to diffuse. This method relies on measuring the density change with time once diffusion of gases has commenced and has been used in other studies.[20,21]

In our study, the Loschmidt cell consists of two chambers of length ($L/2$) through which diffusion occurs. The sample is placed between these two chambers at the location marked as 0. This system is used to measure the effective diffusion coefficient of a mixture containing oxygen. An oxygen sensor is used to measure the change of oxygen concentration with time. With the assumption that the diffusion process follows the transient, 1D Fick's law, the collected data can be fitted to the following equation to find the so-called equivalent diffusion coefficient:

$$C_i = \frac{C_i^{\mathrm{b}}}{2}\mathrm{erfc}\left(\frac{z}{2\sqrt{D_{\mathrm{eq}}t}}\right) \tag{9}$$

where C_i^{b} is the initial concentration of species i in the bottom chamber, and D_{eq} is the equivalent diffusion coefficient. The effective diffusion coefficient is then obtained using an equivalent resistance network as follows:

$$D_{\mathrm{eff}} = \frac{l}{\frac{z}{D_{\mathrm{eq}}} - \frac{z-l}{D_{\mathrm{bulk}}}} \tag{10}$$

where z is the distance from the zero of the axis to the sensor, and l is the thickness of the sample.

Details about the accuracy of this measurement method, the method used for fitting, and equivalent resistance network is given in our previous study.[14] In our previous study, the main focus is on measuring the effective diffusion coefficient in TORAY carbon paper GDL with various wet proofing percentage.

Numerical Formulation

The objective of this study is to determine the effective diffusion coefficient in carbon paper. Much of the experimental measurements available in literature are for TORAY carbon paper. Hence, the modeling domain will be constructed with a realistic morphology similar to that shown in Figure 1. Once the modeling domain is constructed, the concentration distribution of an oxygen−nitrogen gas is simulated in the void regions of the medium.

Mathematical Formulation. The mathematical problem is solved from a macroscopic level. At this level, continuous and differentiable quantities can be determined. The conservation equations are applied in the free void space. Hence, the concentration of gases due to diffusion in the void region of the carbon paper can be obtained according to the second Fick's law of diffusion:

$$\nabla(D_{\mathrm{bulk}}\nabla C_i) = S \tag{11}$$

where C_i is the specie concentration; D_{bulk} is the diffusion coefficient in the free space, also known as the bulk diffusion coefficient; and S is a source term.

Equation 11 must be solved in both the in-plane and through-plane directions to obtain the molar flux. To do so, the concentration at two ends must be specified. The boundary conditions used in this study are listed in Table 1.

Modeling Domain. Two common methods can be used to construct a realistic 3D pore morphology of porous materials. The first such method is the use of 3D volume imaging techniques. This method requires the use of noninvasive experimental techniques, such as X-ray and magnetic resonance, to generate 2D images of the material. The porous material is repeatedly sectioned and imaged automatically. The resultant 2D images are then combined to construct the 3D image of the microstructure. This technique can be very expensive and time-consuming. The second method, which is often employed, is the use of digitally stochastic models. To do so, the pore distribution and pore size of the microstructure are required and usually obtained using a porosimeter. This technique has been employed by other groups[15,17,18,22] and proved to be successful.

(17) Sinha, P. K.; Mukherjee, P. P.; Wang, C. Y. *J Mater Chem.* **2007**, *17*, 3089–3103.
(18) Schulz, V. P.; Mukherjee, P. P.; Becker, J; Wiegmann, A; Wang, C. Y. *ECS Trans.* **2006**, *3*, 1069–1075.
(19) Mukherjee P. P., Wang C. Y. Polymer electrolyte fuel cell modeling - a Pore scale perspective. In: *Progress in Green Energy*; Li, X. Ed.; Springer: New York, 2009; pp 185−228.
(20) Astrath, N. G. C.; Shen, J.; Song, D.; Rohling, J. H.; Astrath, F. B. G.; Zhou, J.; Navessin, T.; Liu, Z. S.; Gu, C. E.; Zhao, X. J. *Phy. Chem. A.* **2009**, *113*, 8369–8374.
(21) Rohling, J. H., Shen, J., Wang, C., Zhou, J., Gu, C. E., 2007. *Appl. Phy. B.* **2007**:*87*:355−362.
(22) Jaganathan, S; Tafreshi, H. V.; Pourdeyhimi, B. *Sep. Sci. Techol.* **2008**, *43*, 1901–1916.

Table 1. Boundary Conditions

boundary	through-plane (z-direction)	in-plane (x-direction)
$z = 0$	$C_i(z = 0) = C_{in}^{z}$ [a]	symmetry boundary condition
$z = 180$	$C_i(z. = 180) = C_{out}^{z}$ [b]	symmetry boundary condition
$x = 0$	symmetry boundary condition	$C_i(x = 0) = C_{in}^{x}$ [c]
$x = 180$	symmetry boundary condition	$C_i(x = 180) = C_{out}^{x}$ [d]
other boundaries	symmetry boundary condition	symmetry boundary condition

[a] Inlet concentration in the z-direction. [b] Outlet concentration in the z-direction. [c] Inlet concentration in the x-direction. [d] Outlet concentrations in the x-direction.

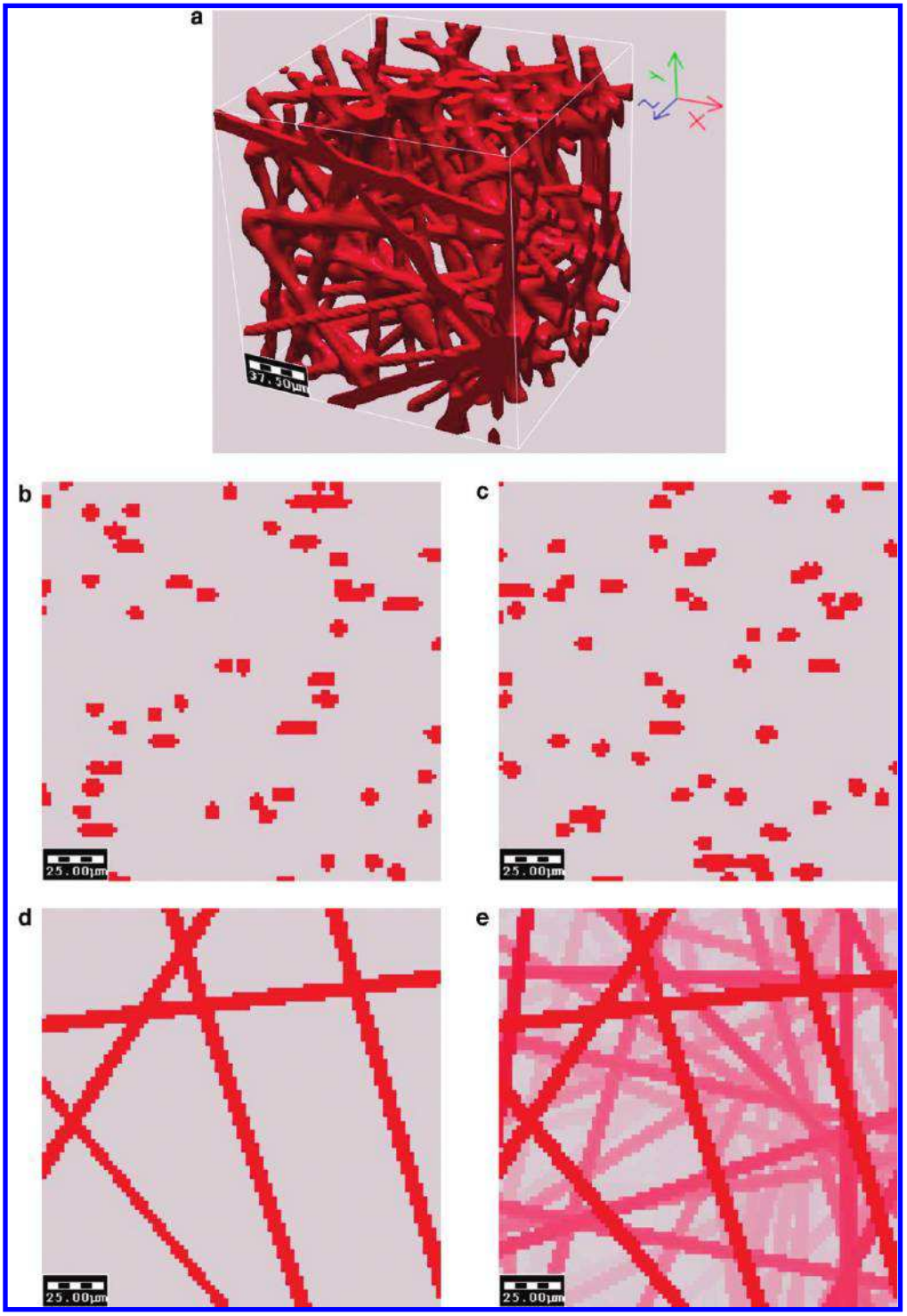

Figure 5. Reconstruction of TORAY carbon paper with 90% porosity. Views: (a) 3D; (b) xz-plane; (c) yz-plane (d) xy-plane; (e) stacked fibers in the xy-plane.

Table 2. Mathematical Models

reference	model	type
Bruggeman[4]	$D_{\text{eff}} = \varepsilon^{1.5} D_{\text{bulk}}$	effective medium approximation
Neale and Nader[5]	$D_{\text{eff}} = \left(\frac{2\varepsilon}{3-\varepsilon}\right) D_{\text{bulk}}$	effective medium approximation
Tomadakis and Sotirchos[6]	$D_{\text{eff}} = \varepsilon\left(\frac{\varepsilon-0.037}{1-0.037}\right)^{0.661} D_{\text{bulk}}$	percolation theory
Nam and Kaviany[7]	$D_{\text{eff}} = \varepsilon\left(\frac{\varepsilon-0.11}{1-0.11}\right)^{0.785} D_{\text{bulk}}$	percolation theory
Das et al.[8]	$D_{\text{eff}} = \left(1-\left(\frac{3(1-\varepsilon)}{3-\varepsilon}\right)\right) D_{\text{bulk}}$	effective medium approximation

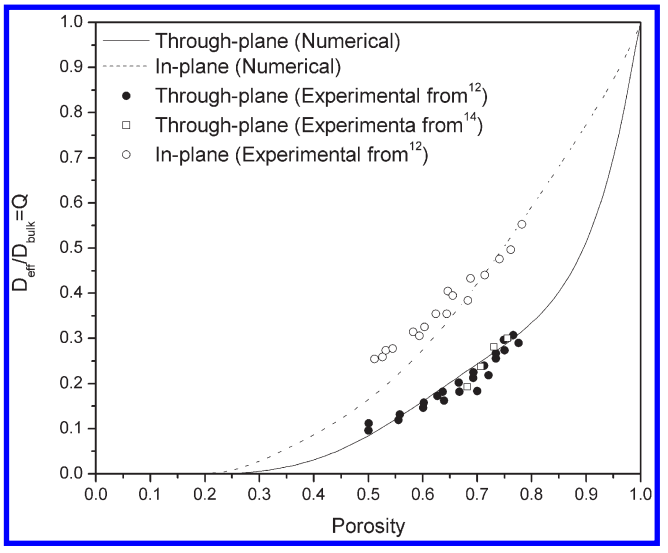

Figure 6. Numerical results of the in-plane and through-plane diffusibility of gases in carbon paper.

In this study, the microstructure of TORAY carbon paper is reconstructed using the stochastic models following the procedure developed by Schladitz et al.[16] Their method relies on knowing the microstructure of carbon paper using 2D cross sectional images. After acquisition of these images, the model geometry is reconstructed based on stochastic methods by fitting model parameters. The geometric characteristics of the microstructure are determined and the parameters of the model are chosen such that the characteristic properties of carbon paper (porosity, fiber radius, and distribution) are presented correctly. Further, other characteristic properties, such as the anisotropy, of carbon paper are also determined. This method also allows for the addition of the carbon composite binder. In order to be able to use this method to obtain the structure of carbon paper, the following assumptions are made: (1) The fibers are considered to be cylindrical, with a constant radius and are infinitely long. (2) The fibers are allowed to overlap. (3) According to the fabrication process of carbon fiber, the fiber system is isotropic in the material plane. In this case, the material plane is defined as the *xy*-plane.

With these assumptions, the directional distribution of the geometry can be obtained. Schladitz et al.[16] suggested that a stationary Poisson line process with a one-parametric directional distribution can be used. The centers defined can be then used as the centers of cylindrical fibers. The cross section of these cylindrical fibers can be either elliptical or circular. In this study, the fibers are taken to have circular cross sections.

In this study, the GeoDict code from ITWM[23] is employed to construct the modeling domain. This code is developed

(23) Fraunhofer ITWM, Department Flow and Complex Structures. *GeoDict*. Available from: http://www.geodict.com, 2005.

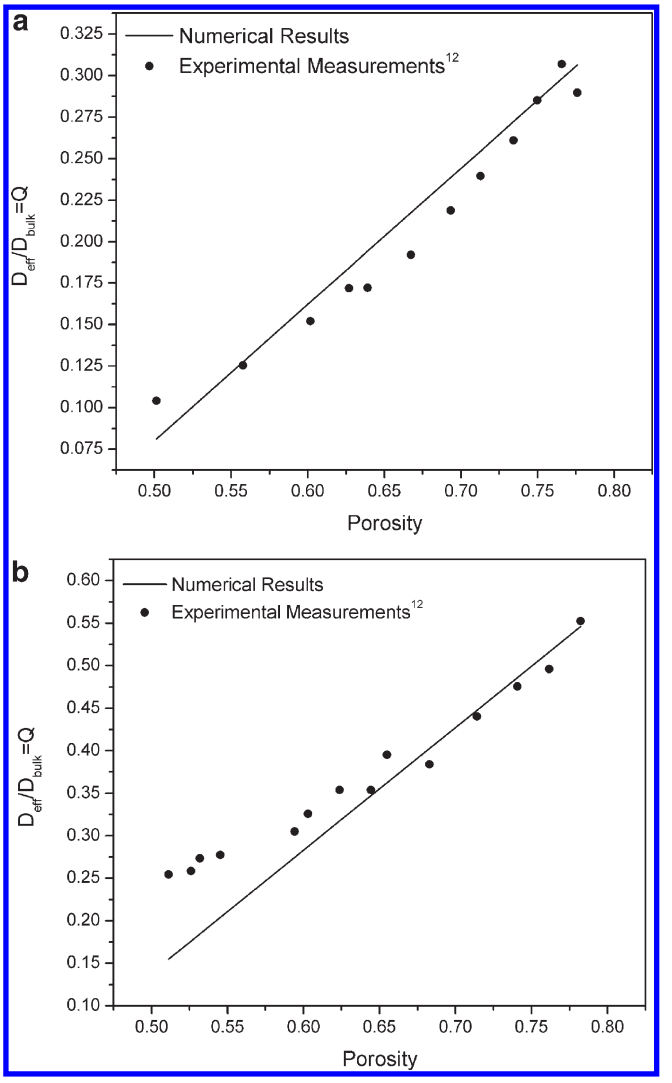

Figure 7. Comparison between the present numerical results and experimental data by Kramer et al.[14] for the porosity range of $0.5 \leq \varepsilon < 0.77$. (a) Through-plane direction; (b) in-plane direction.

using the model by Schladitz et al.[16] A sample mesh of fibers for a carbon paper sample with a 90% porosity is shown in Figure 5. The total volume of this sample is 180 μm × 180 μm × 180 μm. The thickness of TORAY carbon paper ranges from 110 to 400 μm. The effective diffusion coefficient should be independent of this thickness. The fibers are infinitely long with a circular cross section having a radius of 7μm. The total number of grid points is 761 400 (void region + fibers). The number of grid points for the void region depends on the total porosity of the structure.

Figure 5 indicates that the modeling domain is highly anisotropic. As mentioned earlier, the fibers are parallel to the *xy*-plane. Structural similarities between the digitally

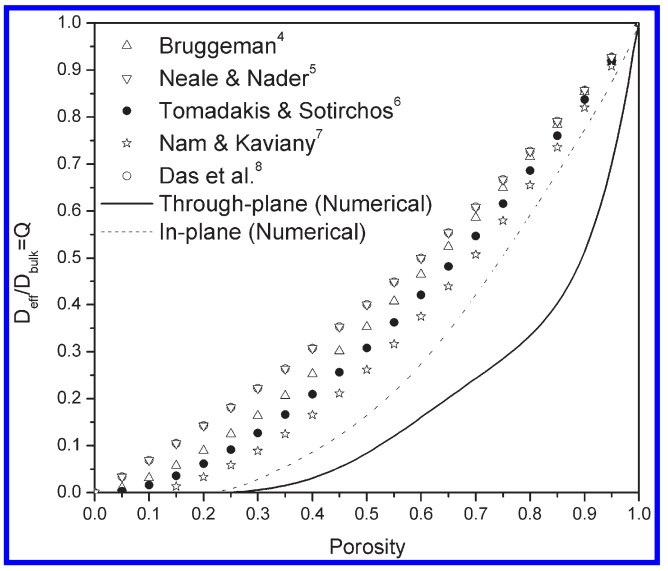

Figure 8. Comparison of the diffusibility evaluated numerically and using the models available (see Table 2 for these models).

constructed TORAY paper and the real structure are apparent once Figures 1a and 5e are compared. It should be pointed out that the presence of a binding agent is ignored in this study. The focus of this study is to investigate the relationship between the porosity and the effective diffusion coefficient. GeoDict requires the user to specify an anisotropic parameter, β, for the structure. According to the model used in GeoDict, the anisotropic parameter describes the distribution of fibers in the xy plane. In the case of carbon paper, β must be larger than 1. An increasing β results in fibers that are parallel to the xy-plane. For the purpose of this study, the value of β was set using the experimental data available in literature for the effective diffusion coefficient through TORAY carbon paper. β equals 10 000 in this study and the porosity is varied; generating various meshes.

Determination of the Effective Diffusion Coefficient. In this study, there are no chemical reactions through which the species can be generated or consumed; thus, the source term is equal to zero in eq 11. With the source term being equal to zero, eq 11 yields a unique solution for the boundary conditions given in Table 1. Using the solution of eq 11, the average diffusive flux can be evaluated as:

$$j = \frac{1}{A}\int_A -D_{\text{bulk}}\,\vec{n}\,\nabla C_i \mathrm{d}A \qquad (12)$$

where j is the average the diffusive flux over a cross section that is normal to the diffusive flux, and A is the surface area over which the flux is evaluated. Once j is obtained, the effective diffusion coefficient can be found.

Prior to solving for the effective diffusion coefficient, it is important to ensure that the solution has converged properly. j must be equal at different cross sections. The value of j is evaluated at the inlet, outlet, and mid section. Further, a residual of 10^{-8} is used as the convergence criteria. Once j is obtained, the effective diffusion coefficient can be calculated as follows:

$$D_{\text{eff}} = \frac{j}{\left(\frac{C_{\text{in}} - C_{\text{out}}}{t}\right)} \qquad (13)$$

where t is equal to 180 μm in this study for both the in-plane and through-plane directions. The effective diffusion coefficient should be independent of t. Hence, to ensure the accuracy of the numerical results, a parametric study was carried out.

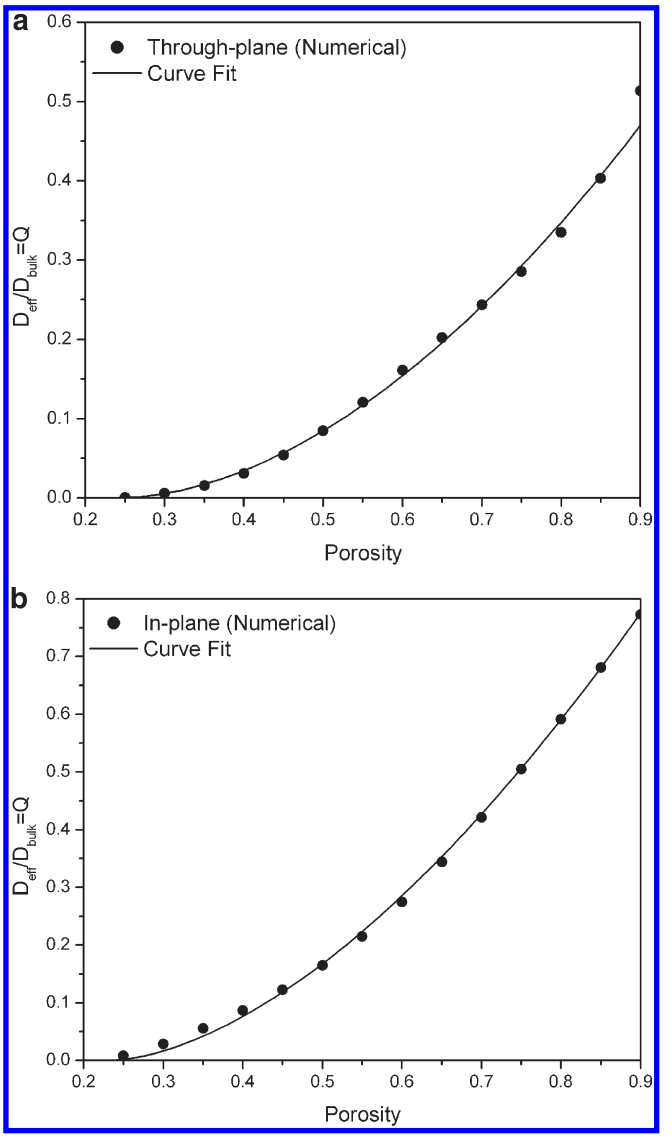

Figure 9. Comparison between the present numerical results and the curve fit from eq 15 for the diffusibility in the (a) through-plane direction; (b) in-plane direction.

Numerical Procedure. GeoDict is used to generate the mesh of carbon paper for various porosity values; porosity range of $0.25 \leq \varepsilon \leq 0.95$ for a total of 15 meshes. The generated meshes are imported into the commercial CFD solver Fluent (6.3.26). This package is based on a finite volume method. Once the mesh is imported into Fluent, eq 11 is solved in the void regions. Due to the anisotropic nature of the carbon paper, the effective diffusion coefficient must be found for three directions, x, y, and z. The effective diffusion coefficient is expected to be the same in the x- and y-directions, also referred to as the in-plane direction, due to the similarity in fiber distribution; (see Figures 5b and 5c). The through-plane direction is in the z-direction. Consequently, eq 11 must be solved twice to obtain the effective diffusion coefficient in both directions. A user-defined-scalar discretized using a second-order finite volume approach with double precision is used to solve the governing equation (eq 11) in this study.

Table 3. Fitting Parameters for Equations 15 and 18

Fitting Parameters for Equation 15					
direction	A	ε_p	α	R^2	validity range
through-plane	1.01 ± 0.02	0.24 ± 0.02	1.83 ± 0.07	0.997	$\varepsilon_p \le \varepsilon < 0.9$
in-plane	1.53 ± 0.01	0.23 ± 0.01	1.67 ± 0.04	0.999	
Fitting Parameters for Equation 18					
direction	A	B	C	R^2	validity range
through-plane	2.76 ± 0.00	3.00 ± 0.03	1.92 ± 0.01	0.998	$0.33 \le \varepsilon < 1$
in-plane	1.72 ± 0.02	2.07 ± 0.02	2.11 ± 0.01	0.999	

Results

Using the numerical method described above, the diffusibility of gases through carbon paper is found. The diffusibility is defined as the ratio between the effective diffusion and bulk diffusion coefficients as given below:

$$Q = \frac{D_{\text{eff}}}{D_{\text{bulk}}} \tag{14}$$

where Q is the diffusibility.

The structure of carbon paper is anisotropic; hence, the diffusion of species is directionally dependent. In this study, the diffusion is simulated in both the in-plane and through-plane directions to obtain the corresponding diffusion coefficients. The results of the numerical simulation for the in-plane and through-plane diffusibility are given in Figure 6.

The anisotropic nature of the carbon paper is found to have an effect on the diffusion process. Hence, the assumption that the gas diffusion layer of a PEM fuel cell is isotropic is not valid. Further, it is seen that the in-plane diffusion of gases is faster than that in the through-plane direction. This finding is consistent with the structure of the carbon paper. The diffusion resistance is higher in the through-plane direction due to the arrangement of fibers. This implies that the use of the anisotropic carbon paper can help increase the overall diffusion magnitude of gases in the GDL. Finally, a porosity value, ε_p, at which the effective diffusion coefficient becomes zero exists and is in the range $0.2 < \varepsilon < 0.3$. The existence of the threshold porosity implies that the fibers are packed in such a way prohibiting the diffusion process from occurring. This analogy is similar to sphere packing.

To verify the accuracy and validity of the numerical method, the results of the numerical model are compared to experimental data obtained from refs 12 and14. The experimental result taken from the study by Zamel et al.[14] was obtained for a TORAY carbon paper (TPGH-120) with various Teflon treatment percentages. TORAY carbon paper (TPGH-60) was used to obtain the experimental data for the study by Kramer et al.[12] Although the experimental data by the two studies are obtained using two different samples, the measurements are still comparable since the samples are manufactured by the same company using the same technique. The only difference between the two samples is their thickness.

Experimental data is not available for the entire porosity range of $0 \le \varepsilon \le 1$ simply because carbon paper is not available commercially for that range. The porosity range for untreated carbon paper, which is available in market, is $0.75 \le \varepsilon \le 0.9$. With the addition of Teflon treatment, the lower limit of this porosity range can be decreased to 0.65. Kramer et al.[12] compressed their carbon paper samples during measurements in order to obtain an even lower porosity range. The compressive force used was studied carefully to ensure that the carbon fibers do not fracture. A good agreement between the numerical and measured results of Kramer et al.[12] is seen; refer to Figure 7. For the in-plane diffusibility, the numerical results deviate from the measured data at the low porosity range. This deviation could be due to compressing the carbon paper during measurements to obtain the desired porosity. No error range has been reported for the measured data making it difficult to further understand this difference. To the authors' knowledge, the measurements in ref 12 are the only available measurements; hence, it is not possible to carry on further comparisons.

As mentioned earlier, the overall objective of this study is to obtain a correlation for estimating the effective diffusion coefficient in the gas diffusion layer of PEM fuel cells. In order to understand the importance of this correlation, a comparison between the available correlations/models and the results of the numerical results of this study should be considered. This comparison is given in Figure 8, and the difference between the diffusibility evaluated numerically and that using the models available is shown to be significant.

From the comparison, it is immediately obvious that all the available correlations overpredict the diffusibility in the GDL in both, in-plane and through-plane, directions. Overpredicting the mass diffusion through the GDL can result in underestimating the mass transport limitations in the layer, especially at high current densities. Underestimating the limitations also occurs due to ignoring the direction dependency of the diffusibility. It is obvious that the through-plane diffusibility is much lower than the in-plane diffusibility. Equating the two will result in inaccurate simulations of the mass diffusion in the GDL.

It is also interesting to note that there are some obvious differences between the two types of correlations. The percolation theory requires that a percolation threshold $\varepsilon_p > 0$ exists. This is, however, not required for the effective medium approximation, and in turn it assumes that diffusion in a porous medium can occur until the porosity of that medium reaches zero. In other words, they assume that $\varepsilon_p = 0$. Thus, it can be argued that correlations developed from an effective medium approximation also satisfy the percolation theory. Finally, studying the numerical and analytical results, the correlation by Nam and Kaviany,[7] eq 7, gives the closest agreement to the numerical results.

The comparison made in Figure 8 raises the need for obtaining more accurate correlations for the in-plane and through-plane diffusibility in the GDL. In reality, carbon paper can be obtained for a porosity range of $0.75 \le \varepsilon \le 0.9$. Once the fuel cell is fully assembled, due to compression, the porosity of the GDL is decreased. For optimal cell performance, the porosity of the compressed GDL should be in the range of 0.4−0.5. The GDL is not only responsible for fluid transport, but also for electron transport. A very porous GDL

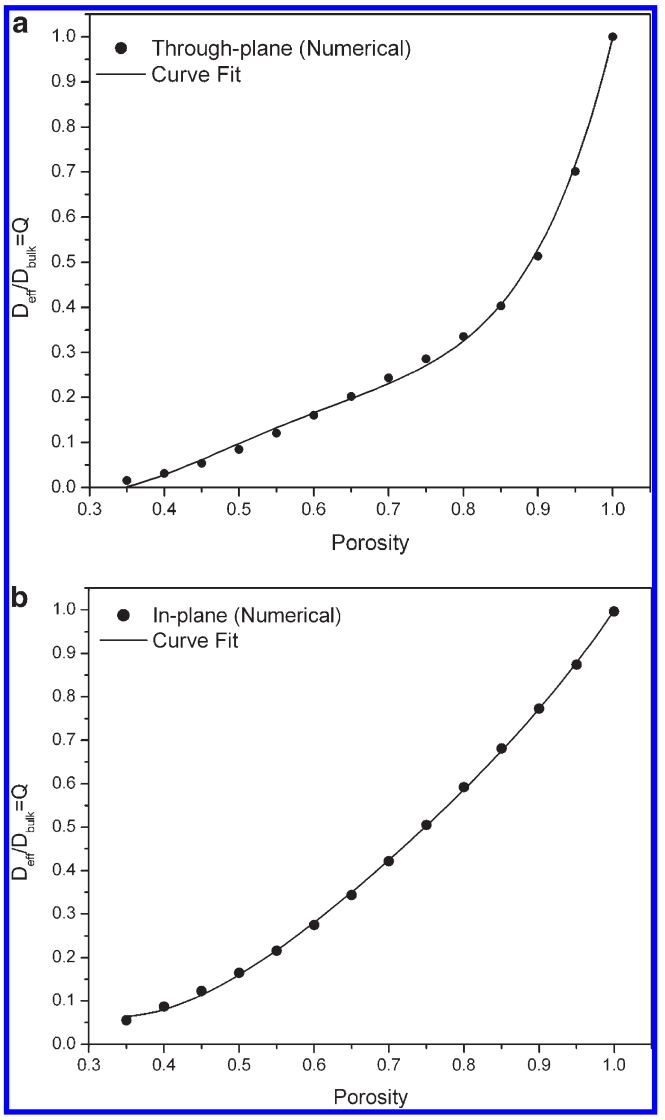

Figure 10. Comparison between the present numerical results and the curve fit from eq 18 for the diffusibility in the (a) through-plane direction; (b) in-plane direction.

can in turn result in poor electron transfer and poor fluid transport occurs due to a low porosity GDL. Thus, in this study, an expression for the through-plane and in-plane diffusibility for the porosity range $\varepsilon_p \leq \varepsilon < 0.9$ is developed. Studying the trend of the results, the percolation theory is used to fit the numerical results as follows:

$$\frac{D_{\text{eff}}}{D_{\text{bulk}}} = A(\varepsilon - \varepsilon_p)^{\alpha} \tag{15}$$

where A is a fitting parameter, ε is the porosity of the GDL, ε_p is the porosity threshold, and α is an empirical constant.

The curve fit for the porosity range $\varepsilon_p \leq \varepsilon < 0.9$ is illustrated in Figure 9. A very good agreement between the fitted results and the numerical results is shown. The values for A, ε_p, and α for the through-plane and in-plane directions are given in Table 3 along with the errors and the values of R^2. R^2 is the coefficient of determination and is calculated as:

$$R^2 \equiv 1 - \frac{\text{SS}_{\text{err}}}{\text{SS}_{\text{tot}}} \tag{16}$$

with $\text{SS}_{\text{err}} = \sum_i (y_i - f_i)^2$ as the total sum of squared errors and $\text{SS}_{\text{tot}} = \sum_i (y_i - \bar{y})^2$ is the total sum of squares. The present numerical results are represented by y_i, f_i denotes the diffusibility predicted by the correlation, and $\bar{y}$ is the average value of numerical results for diffusibility.

In this study, a second correlation is developed for the porosity range $0.33 \leq \varepsilon < 1$. The expression for the diffusibility suggested by Das et al.[8] in eq 5 is used for the curve fit. The function $f(\varepsilon)$, which will be used to fit the data, is expressed in the form of:

$$f(\varepsilon) = \varepsilon A \cosh(B\varepsilon - C) \tag{17}$$

where A, B, and C are fitting parameters. Thus, curve fit to be used for the in-plane and through-plane diffusibility is:

$$\frac{D_{\text{eff}}}{D_{\text{bulk}}} = 1 - \varepsilon A \cosh(B\varepsilon - C)\left(\frac{3(1-\varepsilon)}{3-\varepsilon}\right) \tag{18}$$

Using eq 18, the fitted curves for the through-plane and in-plane diffusibility are given in Figure 9. The corresponding fitting parameters along with the associated errors and the value of R^2 are given in Table 3.

Good agreement between the numerical results and those fitted by eq 18 is shown in Figure 10. Finally, it should be pointed out that the correlations developed in this study are only applicable for TORAY carbon paper with no binding agent. The effect of binding agent on the effective diffusion coefficient through TORAY carbon paper will be investigated in a later study.

Conclusions

In this study, numerical simulation of the diffusion process using the real 3D structure of the GDL of PEM fuel cells is used to estimate the effective diffusion coefficient for different porosity values. The effective diffusion coefficient in the in-plane and through-plane directions is determined. Using the results of the numerical simulation, correlations for the effective diffusion coefficient in both, in-plane and through-plane, directions are found for two different porosity ranges. It is shown that the existing correlations overestimate the effective diffusion coefficient, which can lead to inaccurate estimation of the mass transport limitations in the GDL. The correlations developed in this study are for TORAY carbon paper with no binding agent. Correlations for the in-plane and through-plane for two porosity ranges ($\varepsilon_p \leq \varepsilon < 0.9$) and ($0.33 \leq \varepsilon < 1$) are proposed.

Acknowledgment. The financial support by the Natural Sciences and Engineering Research Council (NSERC) of Canada is greatly appreciated. The authors would like to thank Jürgen Becker and Andreas Wiegmann from Fraunhofer ITWM for giving them access to the GeoDict code.